New Family of Au-Based Superconductors $AuBa_2Ca_{n-1}Cu_nO_{2n+3}$ ($n = 3, 4$)

E. M. Kopnin,† S. M. Loureiro,‡ T. Asaka, Y. Anan, Y. Matsui, and E. Takayama-Muromachi*

National Institute for Research in Inorganic Materials (NIRIM), 1-1 Namiki, Tsukuba, Ibaraki 305-0044, Japan

Received February 8, 2001. Revised Manuscript Received June 18, 2001

$AuBa_2Ca_2Cu_3O_9$ (Au-1223-Ba) and $AuBa_2Ca_3Cu_4O_{11}$ (Au-1234-Ba), two high-T_c superconductors, were synthesized by high-pressure/high-temperature at 6 GPa and 1250−1300 °C. These phases are the third and fourth members of the $AuBa_2Ca_{n-1}Cu_nO_{2n+3}$ series. The Au-1223-Ba and Au-1234-Ba phases crystallize in an orthorhombic primitive system with the lattice parameters $a = 3.8182(4)$ Å, $b = 3.8555(4)$ Å, and $c = 15.445(2)$ Å, and $a = 3.8266(3)$ Å, $b = 3.8505(3)$ Å, and $c = 18.494(1)$ Å, respectively. The Au-1234-Ba phase showed bulk superconductivity below 99 K. The superconducting transition of the as-grown Au-1223-Ba sample was very broad with a transition temperature of ≈30 K and with a small superconducting volume fraction. The volume fraction increased after the sample was postannealed at 300 °C in O_2 atmosphere.

Introduction

Superconducting layered cuprates have conducting CuO_2 planes separated by charge-reservoir blocks. It has been known that various metal and nonmetal elements can occupy the charge reservoir cation sites. The $5d^8$ Au^{3+} ion usually adopts square-planar coordination due to a very strong Jahn−Teller effect.[1] The ionic radius of Au^{3+} in square-planar coordination is 0.68 Å, a value comparable to that of Cu^{2+} (0.57 Å).[2] This seems to be the motivation of Grenoble researchers to replace copper by gold in the charge reservoir block of orthorhombic $YBa_2Cu_3O_7$. Indeed, they succeeded to synthesize $AuBa_2(Y,Ca)Cu_2O_7$ [Au-1212-Ba-(Y,Ca)] with $T_c = 82$ K at 1.8 GPa.[3] The same group showed that substitution of gold for mercury in $HgBa_2Ca_2Cu_3O_y$ is also possible up to 40% and that the structure retained tetragonal symmetry after the substitution.[4]

Recently, it has been shown that high-pressure synthesis is quite effective for stabilizing cuprate layered structures with various charge-reservoir blocks.[5] Since high pressure stabilizes compounds with low thermal stability at ambient pressure, gold-containing systems seem to be good candidates to be synthesized by this technique.

In the present work, we carried out phase search experiments under 6 GPa for the Au−Ba−Ca−Cu−O system, and found a new $AuBa_2Ca_{n-1}Cu_nO_{2n+3}$ ($n = 3$, 4) superconducting family, and studied the synthesized compounds by X-ray diffraction, high-resolution transmission electron microscopy, dc magnetic susceptibility, and electric resistivity measurements.

Experimental Section

BaO_2, Au (99.9%), Au_2O_3 (86% of Au content), CuO (99.9%), and Ca_2CuO_3 were used as initial reagents for high-pressure synthesis. BaO_2 was prepared by a solution route: H_2O_2 and NH_3 were added to an aqueous solution of $BaCl_2$; then the BaO_2 precipitated was collected by filtration. All these procedures were done under N_2 atmosphere to avoid contamination of CO_2. After it was dried at 150 °C in O_2, the carbon content in BaO_2 was determined by a carbon analyzer (LECO, WR12) to be less than 0.008 wt %. Single-phase Ca_2CuO_3 was prepared from $CaCO_3$ (99.9%) and CuO at 970 °C in air for 1 week with several intermediate grindings. Appropriate amounts of precursors were mixed in an agate mortar and sealed into a gold capsule in a glovebox filled with dried N_2. The mixture was allowed to react in a belt-type high-pressure apparatus at 6 GPa and 1250−1300 °C for 2−3 h, and then was quenched to room temperature. Very careful treatment to avoid carbon contamination was indispensable for the present system. If BaO_2 was handled in air or commercial BaO_2 was used, oxycarbonate series of phases $(Cu,C)Ba_2Ca_{n-1}Cu_nO_{2n+3}$[6] were formed instead of the gold-based phase.

X-ray diffraction (XRD) data were collected using a powder diffractometer (Phillips PW 1800) with Cu Kα radiation. Lattice constants were determined by a least-squares refinement procedure. Electron probe microanalysis (EPMA) was performed using an analyzer (JEOL JXA-8600MX) to determine the cation compositions of the high-pressure phases. High-resolution transmission electron microscopy (HRTEM) observations were carried out for some selected samples with

* Corresponding author.
† STA fellow of NIRIM. On leave from Inorganic Chemistry Department, Moscow State University, Moscow, Vorobyevy Gory 119899, Russia.
‡ Present address: Department of Chemistry, Princeton University, Princeton, NJ 08544.

(1) Wells, A. F. *Structural Inorganic Chemistry*, 4th ed.; Clarendon Press: Oxford, 1975.
(2) Shannon, R. D. *Acta Crystallogr. A* **1976**, *32*, 751.
(3) Bordet, P.; Le Floch, S.; Chaillout, C.; Duc, F.; Gorius, M. F.; Perroux, M.; Capponi, J. J.; Toulemonde, P.; Tholence, J. L. *Physica C* **1997**, *276*, 237.
(4) Bordet, P.; Le Floch, S.; Capponi, J. J.; Chaillout, C.; Gorius, M. F.; Marezio, M.; Tholence, J. L.; Radaelli, P. G. *Physica C* **1996**, *262*, 151.
(5) Takayama-Muromachi, E. *Chem. Mater.* **1998**, *10*, 2686.
(6) Kawashima, T.; Matsui, Y.; Takayama-Muromachi, E. *Physica C* **1994**, *224*, 69.

10.1021/cm010126a CCC: $20.00
Published on Web 08/30/2001

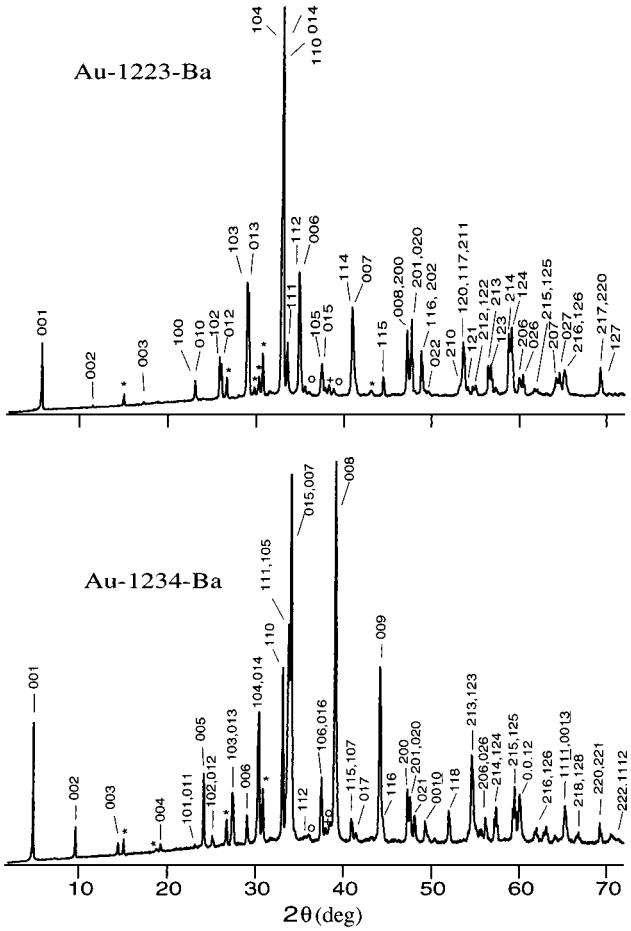

Figure 1. X-ray diffraction patterns for the Au-1223-Ba and Au-1234-Ba samples with $d = 0$. Unidentified peaks are shown by asterisks. CuO and Au impurities are shown by open circles and pluses, respectively.

a microscope (Hitachi H-1500) operating at 800 kV. Magnetic susceptibilities were measured under zero-field-cooling and field-cooling conditions in an applied field of 10 Oe with a DC SQUID magnetometer (Quantum Design, MPMS). Electric resistivity measurements were carried out by the conventional four-probe method with silver paste for electrodes using a physical property measurement system (Quantum Design, PPMS).

Results and Discussion

More than 20 starting mixtures were tested varying the cation ratio and the oxygen content. Among them, samples with starting compositions of $AuBa_2Ca_2Cu_3O_{9+d}$ ($d = 0$, 0.1, 0.2) contained a new orthorhombic phase with $c \approx 15$ Å (hereafter, denoted Au-1223-Ba). The $d = 0$ starting mixture gave the best phase purity for Au-1223-Ba with an XRD pattern in Figure 1. The $AuBa_2Ca_3Cu_4O_{11+d}$ ($d = 0$, 0.1, 0.2) starting mixture originated a new orthorhombic phase with $c \approx 18$ Å (Au-1234-Ba), with the highest phase purity for $d = 0$ as well (XRD pattern in Figure 1). The lattice parameters for Au-1223-Ba and Au-1234-Ba samples with $d = 0$ were $a = 3.8182(4)$, $b = 3.8555(4)$, and $c = 15.445(2)$ Å, and $a = 3.8266(3)$, $b = 3.8505(3)$, and $c = 18.494(1)$ Å, respectively.

Besides the main phases, both samples contained unknown phase(s) whose X-ray peaks are denoted by asterisks in Figure 1 as well as small amounts of CuO and gold metal. The presence of the impurity phases suggests that the real compositions of the orthorhombic phases may differ from the stoichiometric ones of 1:2:2:3 (Au/Ba/Ca/Cu) and 1:2:3:4. To verify this hypothesis, we carried out EPMA measurements of the Au-1223-Ba and Au-1234-Ba phases in samples with $d = 0$. The experimental cation ratios were determined by averaging the data of seven Au-1223-Ba grains and nine Au-1234-Ba grains. The results were 0.9(1):1.91(6):2.10(6):3.1(1) for Au-1223-Ba and 0.8(1):1.9(1):3.1(1):4.2(1) for Au-1234-Ba. In both cases the experimental ratios are close to stoichiometric values. Even though the Au-1234-Ba phase seems slightly Au-deficient and Cu-rich, it is not possible to fully confirm this because of the large experimental uncertainty. The EPMA measurements detected CuO and gold metal in both samples, consistent with their X-ray patterns. In addition, both samples contained a Cu-free unknown phase of "Ca_2BaAuO_y" which probably corresponds to the additional X-ray peaks denoted by asterisks in Figure 1.

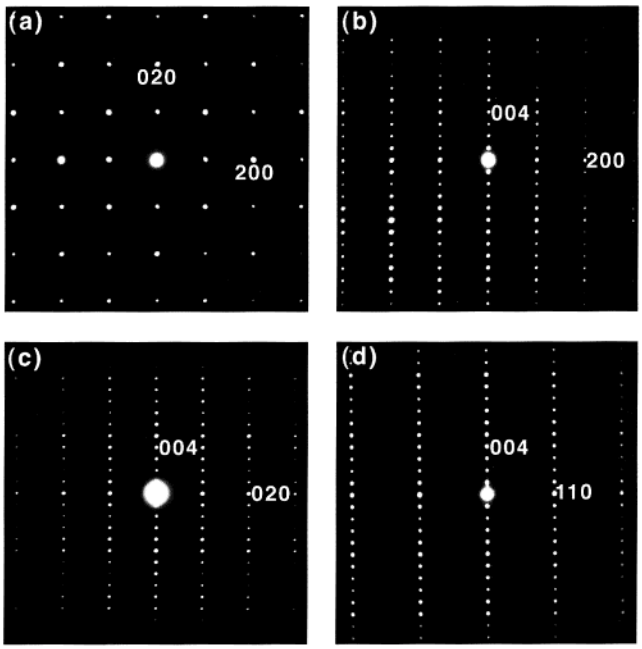

Figure 2. Electron diffraction patterns for the Au-1223-Ba phase taken along the [001] (a), [010] (b), [100] (c), and [1−10] (d) zone axes.

The present Au-1223-Ba and Au-1234-Ba phases are the $n = 3$, 4 members of the homologous series $AuBa_2Ca_{n-1}Cu_nO_{2n+3}$, respectively. Starting mixtures with $AuBa_2Ca_{n-1}Cu_nO_{2n+3}$ ($n = 5$, 6) were tested, expecting higher-order members of Au-1245-Ba and Au-1256-Ba. Oxygen-poor 1234 compositions of $AuBa_2Ca_3Cu_4O_{11+d}$ ($d = -0.1$ and -0.2) were also tested, since a higher-order member sometimes becomes stable under relatively low oxygen pressure.[5] In addition, we extended the high-pressure reaction period up to 6 h. Despite these attempts, peaks assignable to Au-1245-Ba or Au-1256-Ba were not observed at all in XRD patterns.

The Au-1223-Ba and Au-1234-Ba phases were studied by HRTEM. Figure 2 shows electron diffraction patterns of the Au-1223-Ba phase taken along the [001], [010], [100], and [1−10] zone axes. All diffraction spots could be indexed by a primitive orthorhombic lattice consistent with the XRD patterns. No systematic extinction

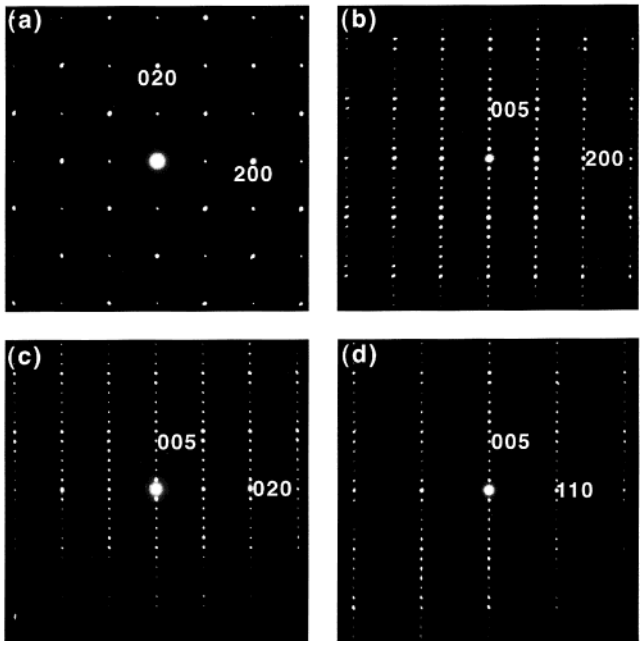

Figure 3. Electron diffraction patterns for the Au-1234-Ba phase taken along the [001] (a), [010] (b), [100] (c), and [1−10] (d) zone axes.

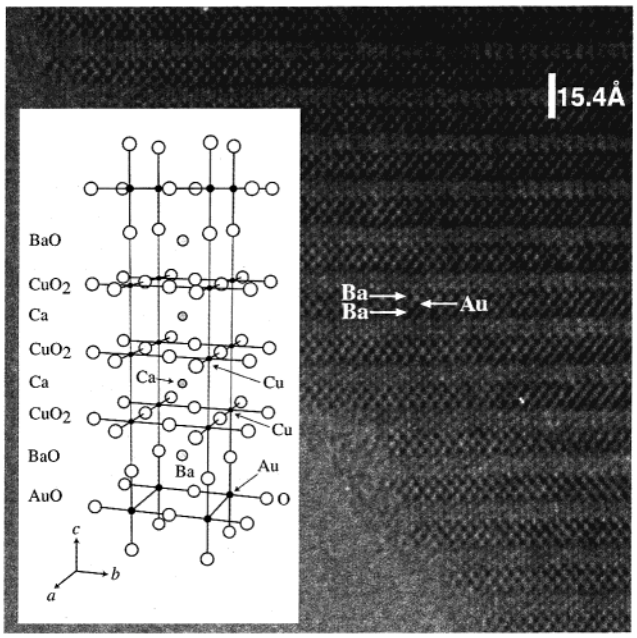

Figure 4. HRTEM image for the Au-1223-Ba phase taken along the [100] zone axis. The inset represents a schematic structure model for the Au-1223-Ba phase.

was observed, suggesting a space group *Pmmm* or *Pmm*2. Extremely weak additional spots corresponding to a superlattice cell with $b_s = 2b$ were sometimes observed in the electron diffraction patterns. Although the same type of superstructure was reported for the Au-1212-Ba-(Y,Ca) phase,[3] the superstructure spots are much less intensive in the case of Au-1223-Ba. The electron diffraction patterns of the Au-1234-Ba phase are shown in Figure 3. The patterns are consistent with a primitive orthorhombic lattice with the space group *Pmmm* or *Pmm*2, as was the case for Au-1223-Ba. Differing from those observed in the electron diffraction patterns of Au-1223-Ba, no superlattice spots were observed for the Au-1234-Ba phase.

Figure 4 presents a HRTEM image for the Au-1223-Ba phase projected along the *b*-axis. The image reveals an M-1223-type structure with stacking of the planes along the *c*-axis, BaO−AuO−BaO−CuO_2−Ca−CuO_2−Ca−CuO_2. In the inset of Figure 4, a schematic structure model is shown according to the lattice image. For the Au-1212-Ba-(Y,Ca) phase, it was reported that a Au−O zigzag chain is formed with doubling of the *b*-axis and lowering of the symmetry to *P*2/*m* from *P*4/*mmm*,[3] instead of the linear one shown in Figure 4. Weak extra electron diffraction spots observed for Au-1223-Ba reveal local formation of the superstructure of $b_s = 2b$, suggesting the formation of a similar zigzag chain in the present system. We have succeeded in obtaining single crystals of Au-1223-Ba, and single-crystal X-ray analysis is in progress to elucidate the structural details including the arrangement of the oxygen atoms in the Au−O plane.

Several $MA_2Ca_{n-1}Cu_nO_{2n+3}$ [A, alkaline earth; M-12-(n-1)n-A] superconducting families have been reported for trivalent M atoms. They include Tl-12(n-1)n-Ba,[7] B-12(n-1)n-Sr,[8,9] Al-12(n-1)n-Sr,[10] and Ga-12(n-1)n-Sr.[11−13] It is worth noting that all these M atoms belong to the 3A elements of the periodic table and that indium is the only element of column 3A that does not form the M-12(n-1)n-type series. In spite of the fact that trivalent gold has a similar ionic radius to that of indium,[2] it can accommodate itself to the M-site. This fact may be related to the square-planar coordination preference of the gold ion.

In Figure 5, the magnetic susceptibilities for the $AuBa_2Ca_2Cu_3O_{9.0}$ and $AuBa_2Ca_3Cu_4O_{11.0}$ samples are shown. The Au-1234-Ba phase undergoes the superconducting transition at $T_c = 99$ K and has large enough diamagnetism at 5 K. On the other hand, in the as-grown Au-1223-Ba sample, the decrease of the magnetic susceptibility starts at ≈90 K but both Meissner and shielding fractions are very small even at 5 K.

To change the hole concentration of Au-1223-Ba, the sample was postannealed for 2 h at 300 °C under oxygen atmosphere. According to the thermogravimetric analysis, the weight decrease by the postannealing is ≈0.13%, which corresponds to removal of ≈0.07 oxygen atoms or a decrease of 0.14 holes per unit formula. After the postannealing, the superconducting volume fraction increased noticeably, as shown in Figure 5. However, the superconducting transition is still very broad. Weak diamagnetism is seen below ≈90 K in the postannealed sample, but the main transition occurs around 30 K, which appears to be the T_c of Au-1223-Ba. The ≈90 K

(7) Sheng, Z. Z.; Hermann, A. M. *Nature* **1988**, *332*, 55.

(8) Takayama-Muromachi, E.; Matsui, Y.; Kosuda, K. *Physica C* **1995**, *241*, 137.

(9) Kawashima, T.; Matsui, Y.; Takayama-Muromachi, E. *Physica C* **1995**, *254*, 131.

(10) Isobe, M.; Kawashima, T.; Kosuda, K.; Matsui, Y.; Takayama-Muromachi, E. *Physica C* **1994**, *234*, 120.

(11) Vaughey, J. T.; Thiel, J. P.; Hasty, E. F.; Groenke, D. A.; Shtern, C. L.; Poeppelmeier, K. R.; Dabrowski, B.; Hinks, D. G.; Mitchell, A. W. *Chem. Mater.* **1991**, *3*, 935.

(12) Dabrowski, B.; Radaelli, P.; Hinks, D. G.; Mitchell, A. W.; Vaughey, J. T.; Groenke, D. A.; Poeppelmeier, K. R. *Physica C* **1992**, *193*, 63.

(13) Takayama-Muromachi, E.; Isobe, M. *Jpn. J. Appl. Phys.* **1994**, *33*, L1399.

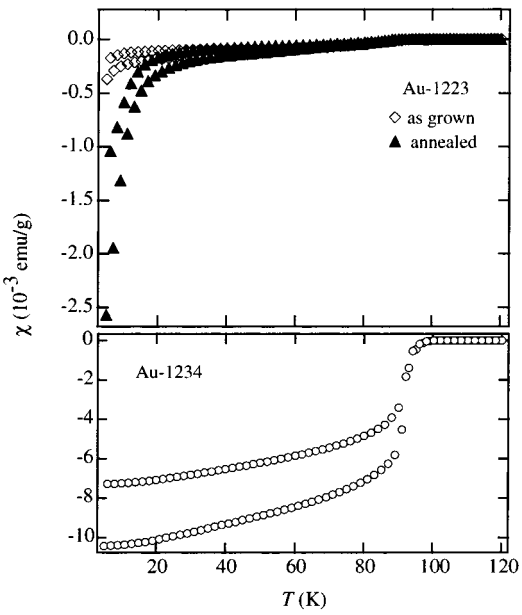

Figure 5. Magnetic susceptibility data for the Au-1223-Ba and Au-1234-Ba samples. The larger diamagnetic effect is from the zero-field-cooling method while the smaller one is from the field-cooling method.

transition is likely due to the Au-1234-Ba phase, although undetected by XRD. These results may suggest that the as-grown Au-1223-Ba phase lies in the overdoped state of holes.

The electric resistivities of Au-1223-Ba and Au-1234-Ba are given in Figure 6. The normal-state temperature dependencies reveal the metallic nature for both phases. In Au-1234-Ba, the onset temperature is 108 K and zero-resistivity is attained at 93 K. As expected from the magnetic data, two-step superconducting transitions were observed for the as-grown Au-1223-Ba sample at 86 K and ≈40 K with a zero-resistivity temperature of 13 K. Both phases indicate a large residual resistivity with extrapolation of the normal-state resistivity to zero temperature. Impurity phases contained in both samples could be a reason for the large residual resistivity. We need to obtain a single-phase sample to elucidate this problem, and such an attempt is in progress.

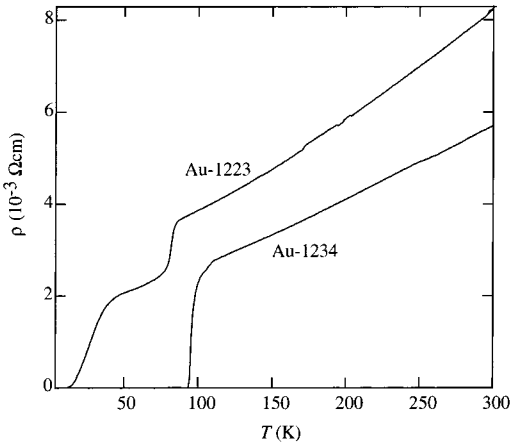

Figure 6. Electric resistivity data for the Au-1223-Ba and Au-1234-Ba samples with $d = 0$.

Conclusions

Two members of a new Au-based $AuBa_2Ca_{n-1}Cu_nO_{2n+3}$ family with $n = 3, 4$ (Au-1223-Ba and Au-1234-Ba) were synthesized by high-pressure/high-temperature conditions at 6 GPa and 1250−1300 °C. The X-ray diffraction and high-resolution transmission electron microscopy measurements show a M-12(n-1)n-type structure with $BaO-AuO-BaO-CuO_2-(Ca-CuO_2)_{n-1}$ stacking of planes along the *c*-axis. The Au-1234-Ba phase showed bulk superconductivity below $T_c = 99$ K. The superconducting transition of Au-1223-Ba is very broad with a small volume fraction even at 5 K. Some oxygen was lost from the Au-1223-Ba phase after postannealing at 300 °C in O_2, which leads to a noticeable increase of the superconducting volume fraction. This result suggests an overdoped state of carriers in the as-grown Au-1223-Ba

Acknowledgment. The authors would like to thank M. Akaishi and S. Yamaoka for helpful suggestions on high-pressure synthesis, K. Kosuda for the EPMA measurements, and S. Takenouchi for the carbon analysis. This work was supported by the Multi-Core Project and Special Coordination Funds of the Science and Technology Agency of the Japanese Government.

CM010126A